

Semi-active friction dampers for seismic control of structures

Jagadish G. Kori* and R. S. Jangid‡

Department of Civil Engineering, Indian Institute of Technology Bombay, Powai, Mumbai - 400 076, India

(Received July 16, 2006, Accepted January 31, 2008)

Abstract. Semi-active control systems have attracted a great deal of attention in recent years because these systems can operate on battery power alone, proving advantageous during seismic events when the main power source of the structure may likely fail. The behavior of semi-active devices is often highly non-linear and requires suitable and efficient control algorithm. This paper presents the comparative study and performance of variable semi-active friction dampers by using recently proposed predictive control law with direct output feedback. In this control law, the variable slip force of semi-active variable friction damper is kept slightly lower than the critical friction force, which allows the damper to remain in the slip state during an earthquake, resulting in improved energy dissipation capability. This control algorithm is able to produce a continuous and smooth slip forces for a variable friction damper. The numerical examples include a structure controlled with multiple variable semi-active friction dampers and with multiple passive friction dampers. A parameter, gain multiplier defined as the ratio of damper force to critical damper control force, is investigated under four different real earthquake ground motions, which plays an important role in the present control algorithm of the damper. The numerically evaluated optimum parametric value is considered for the analysis of the structure with dampers. The numerical results of the variable friction dampers show better performance over the passive dampers in reducing the seismic response of structures.

Keywords: structural control; semi-active control; variable friction damper; earthquake; control algorithm.

1. Introduction

The main aim in seismic control of structures is to dissipate energy from earthquakes and reduce vibration in the structures, thereby reducing the human and material losses. This is achieved by installation of special seismic protection control systems that ensure essentially elastic behavior of the structure during a major earthquake. A variety of control systems have been proposed and implemented which can be classified as passive, active and semi-active systems (Housner, *et al.* 1997, Soong and Dargush 1997, Soong and Spencer 2002). Passive control systems impart forces on the structure by reacting to the localized motion of the structure, primarily acting to dissipate the vibratory energy in the structural system. These systems are now widely accepted as a viable means of reducing the responses of a structure. However, there is a limitation for passive control systems, as they cannot adapt to varying loading or excitation conditions. Thus, passive control systems may perform well when subjected to the loading conditions for which they were designed, but may not be quite effective in

*Research Scholar

‡Professor, Corresponding author, E-mail: rsjangid@civil.iitb.ac.in

other situations. On the other hand, active control systems operate by using external energy supplied by actuators to impart forces on the structure, generally depending on a sizeable power supply. The appropriate control action is typically determined based on measurements of the structural responses (Soong and Constantinou 1994, Soong 1990). However, active control systems require sizeable power supplies and large control forces may make them quite costly to install and maintain. In addition, the availability of large external power supply during extreme seismic event is also questionable. Semi-active control systems offer an alternative to passive and active control devices in structural control. Typically, a semi-active control device is defined as one that cannot increase the mechanical energy in the controlled system, but has properties that can be dynamically varied. Since these devices are adaptable, they are expected to be quite effective for structural response reduction over a wide range of loading conditions. A variety of semi-active control devices have been proposed, including variable orifice dampers, variable friction devices, adjustable tuned liquid dampers and controllable fluid dampers (Symans and Constantinou 1999, Yang and Agrawal 2002). These systems have attracted much attention recently because they possess the adaptability of active control systems and operate using very low power.

One of the semi-active devices that appear to be particularly promising for seismic protection is variable friction damper (Akbar and Aktan 1995). A friction damper is a displacement-dependent energy dissipation device such that the damper force is independent from the velocity and frequency-content of excitations. A friction damper is activated and starts to dissipate energy when the friction force exerted on the friction interface exceeds the maximum frictional force, otherwise an inactivated damper behave as a regular bracing system. In a passive friction damper, the slip force of the damper is a preset fixed value, so for a given earthquake the damper is activated only when the exerted force exceeds this fixed value, hence the energy dissipation capacity of the damper is not fully utilized. To improve the performance of passive friction dampers, the concept of semi-active friction damper was introduced (Akbar and Aktan 1995, Lu 2004a). A semi-active friction damper is able to adjust its slip force by controlling its clamping force in real-time in response to a structure's motion during an earthquake. A semi-active friction damper is expected to be more effective than a passive damper because of this adaptive nature. The control of semi-active friction dampers requires a feedback control algorithm and on-line measurement of structural response in order to determine the appropriate level of adjustable clamping forces of the dampers.

A few number of semi-active control algorithms for friction-type variable dampers have been proposed in past literature. Akbar and Akean (1995) proposed the control algorithm that determines the next time-step clamping force. Other proposed control laws include the instantaneous optimal control (Feng, *et al.* 1993), bang-bang control (Kannan, *et al.* 1995), modulated homogenous control (Inaudi 1997), linear quadratic regulator (Sadek and Mohraz 1998), modal control (Lu and Chung 2001), friction-force incremental control (Xu, *et al.* 2001), combined viscous and Reid control (Chen and Chen 2002), predictive control (Lu 2004a) and linear control (Lu, *et al.* 2004b). The investigation on predictive control algorithm method (Lu 2004a) was focused on the predicting the critical friction force, but the evaluation of optimal gain multiplier, which is the ratio of damper force to critical control force based on the different configuration of damper locations under different earthquake loadings are so far not investigated. Thus, it will be interesting to investigate the optimal gain multiplier and its effectiveness with variable semi-active friction damper for seismic control of structures subjected to different types of earthquake ground motions. The seismic response of five and ten-story structures equipped with variable friction damper is investigated in this paper. The specific objectives of the present numerical study are to (i) identify a suitable semi-active control law parameter, so that it can

control very effective and reduce the displacement and acceleration response of the structures, (ii) investigate the effect of variation in the gain multiplier of damper force on the controlled structural responses, (iii) identify the optimal value of gain multiplier for the best possible structural control configurations with different damper deployments, (iv) investigate the hysteretic energy dissipation behavior of the damper and (v) to investigate numerically the feasibility and efficiency of variable friction damper in comparison with the passive friction damper.

2. Modeling of structure with variable friction damper

Consider a seismically excited n -story structure controlled with r semi-active friction dampers as shown in Fig. 1(a). A friction damper, in general, consists of two bodies, which slide with respect to each other subjected to a controllable clamping force N_i , generating a dissipative force proportional to the clamping force, $N_i(\geq 0)$ and the coefficient of friction, between the surfaces. The mathematical model of semi-active variable friction damper is shown in Fig. 1(b). The mass, stiffness and displacement of the i^{th} floor relative to the ground are denoted by $m_{s,i}$, $k_{s,i}$ and $x_i(t)$, respectively. The stiffness of bracing and controllable clamping force of the i^{th} dampers are denoted by $k_{b,i}$ and N_i , respectively. The governing equations of motion for n -degrees-of-freedom controlled building structure model subject to seismic excitations can be written as

$$\mathbf{M}\ddot{\mathbf{x}} + \mathbf{C}\dot{\mathbf{x}} + \mathbf{K}\mathbf{x} = \mathbf{D}\mathbf{u} - \mathbf{M}\mathbf{1}\ddot{x}_g \tag{1}$$

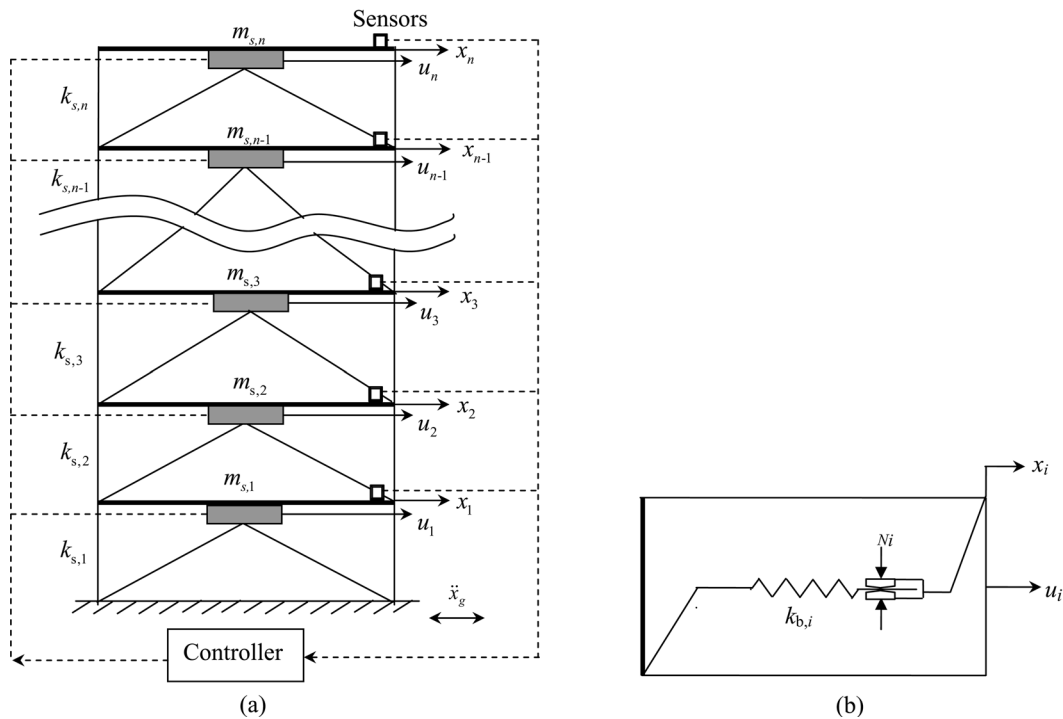


Fig. 1 (a) Schematic diagram of a structure with variable friction dampers and control feedback system (b) Model of Semi-active Friction Damper

where \mathbf{x} is displacement vector, $\dot{\mathbf{x}}$ and $\ddot{\mathbf{x}}$ represent the first and second time derivatives of \mathbf{x} , respectively; \mathbf{u} and \ddot{x}_g are control force vector and the ground acceleration, respectively; \mathbf{M} , \mathbf{C} , and \mathbf{K} are mass, damping and stiffness matrices, respectively; and \mathbf{D} and $\mathbf{1}$ are the control force matrix and influence coefficient vector, respectively.

Eq. (1) can be further transformed to state space representation as

$$\dot{\mathbf{z}} = \mathbf{A}\mathbf{z} + \mathbf{B}\mathbf{u} + \mathbf{E}\ddot{x}_g \quad (2)$$

where \mathbf{z} is the state vector of structure, and contains the relative ground displacement and velocity of each floor; \mathbf{A} denotes the system matrix composed of structural mass, damping and stiffness matrices; \mathbf{B} represents the distributing matrices of the control forces; and \mathbf{E} represents the distributing matrices for excitation.

The Eq. (2) is discretized in the time domain and excitation force is assumed to be constant within any time interval and can be written into a discrete-time form (Meirovitch 1990) as

$$\mathbf{z}[k+1] = \mathbf{A}_d\mathbf{z}[k] + \mathbf{B}_d\mathbf{u}[k] + \mathbf{E}_d\ddot{x}_g[k] \quad (3)$$

where k denotes the time step; $\mathbf{A}_d = e^{\mathbf{A}\Delta t}$ represents the discrete-time system matrix with Δt as the time interval. The constant coefficient matrices \mathbf{B}_d and \mathbf{E}_d are the discrete-time counterpart of the matrices \mathbf{B} and \mathbf{E} that may be written as

$$\mathbf{B}_d = \mathbf{A}^{-1}(\mathbf{A}_d - \mathbf{I})\mathbf{B} \quad (4)$$

$$\mathbf{E}_d = \mathbf{A}^{-1}(\mathbf{A}_d - \mathbf{I})\mathbf{E} \quad (5)$$

where \mathbf{I} is the identity matrix.

Let the actual friction force vector be denoted by $\mathbf{u}[k]$ and critical force vector by $\tilde{\mathbf{u}}[k]$, which are reduced to scalars $u[k]$ and $\tilde{u}[k]$. The state of the damper may be either stick or slip condition.

$$\text{a) in the stick state, if } |\tilde{u}[k]| < u_{\max}[k] = \mu N[k] \quad (6a)$$

$$\text{b) in the slip state, if } |\tilde{u}[k]| \geq u_{\max}[k] = \mu N[k] \quad (6b)$$

The clamping force $N_i[k]$ of the damper is kept always slightly less than the critical force $\tilde{u}_i[k]$, so that the damper will remain in the slip state for the entire time history. Based on this concept, the control rule for determining the clamping force of a semi-active damper is (Lu 2004) as

$$N_i[k] = \mathbf{R}_f \frac{|\tilde{u}_i[k]|}{\mu}, \quad 0 \leq \mathbf{R}_f < 1 \quad (\text{for } i = 1-r) \quad (7)$$

where \mathbf{R}_f is a gain multiplier parameter defined as the ratio of damper force to critical damper control force and plays an important role in the present control law. A larger value of \mathbf{R}_f will lead to higher control force, but this does not necessarily guarantee better energy dissipation capacity, the optimum value of \mathbf{R}_f parameter will be seen and obtained by the numerical results shown in the latter section.

3. Friction control law

The effective performance and utilization of the semi-active friction damper strongly depends on the control strategy used. Here, a recently developed predictive control with direct output feedback concept is considered. This method employs the technique of multiple-step feedback (Lu 2004). Let the sensor measurement vector $\mathbf{y}_s[k-1]$ be given by

$$\mathbf{y}_s[k-1] = \mathbf{C}_f \mathbf{z}[k-1] \quad (8)$$

where \mathbf{C}_f is the sensor placement matrix, the dimensions of $\mathbf{y}_s[k-1] \in \mathbf{R}^{q \times 1}$ and $\mathbf{C}_f \in \mathbf{R}^{q \times 1}$. Here q which is the number of sensors deployed in the structure is much less than $2n$. Now by replacing the index k by $(k-2)$ in the Eq. (3) and replacing the index $(k-1)$ by $(k-2)$ in the Eq. (8), the sensor measurement $\mathbf{y}_s[k-2]$ can be

$$\mathbf{y}_s[k-2] = \mathbf{C}_f \mathbf{A}_d^{-1} \mathbf{z}[k-1] - \mathbf{C}_f \mathbf{A}_d^{-1} \mathbf{u}[k-2] - \mathbf{C}_f \mathbf{A}_d^{-1} \mathbf{E}_d \ddot{\mathbf{x}}_g[k-2] \quad (9)$$

Using Eqs. (3) and (8) repeatedly, the sensor measurement vector $\mathbf{y}_s[k-m]$ for the m^{th} preceding time step can be written as

$$\mathbf{y}_s[k-m] = \mathbf{C}_f \mathbf{A}_d^{-(m-1)} \mathbf{z}[k-1] - \sum_{j=1}^{m-1} \mathbf{C}_f \mathbf{A}_d^{-(m-j)} \mathbf{B}_d \mathbf{u}[k-j-1] - \sum_{j=1}^{m-1} \mathbf{C}_f \mathbf{A}_d^{-(m-j)} \mathbf{E}_d \ddot{\mathbf{x}}_g[k-j-1] \quad (10)$$

(for $m \geq 2$)

where the matrix operation $\mathbf{A}_d^a = (\mathbf{A}_d^{-1})^a$ (for $a > 0$).

Substituting the same in Eqs. (8) and (10) (representing $m-1$ equations, for $m \geq 2$), the combined and expanded matrix form is given by

$$\bar{\mathbf{y}}[k-1] = \bar{\mathbf{A}}_d \mathbf{z}[k-1] + \bar{\mathbf{B}}_d \bar{\mathbf{u}}[k-1] + \bar{\mathbf{E}}_d \bar{\mathbf{x}}_g[k-1] \quad (11)$$

where

$$\bar{\mathbf{y}}[k-1] = \begin{Bmatrix} \mathbf{y}_s[k-1] \\ \mathbf{y}_s[k-2] \\ \vdots \\ \mathbf{y}_s[k-m] \end{Bmatrix} \in \mathbf{R}^{qm \times 1} \quad (12)$$

$$\bar{\mathbf{u}}[k-1] = \begin{Bmatrix} \mathbf{u}[k-1] \\ \mathbf{u}[k-2] \\ \vdots \\ \mathbf{u}[k-m] \end{Bmatrix} \in \mathbf{R}^{mr \times 1} \quad (13)$$

$$\bar{\mathbf{x}}_g[k-1] = \begin{Bmatrix} \ddot{\mathbf{x}}_g[k-1] \\ \ddot{\mathbf{x}}_g[k-2] \\ \vdots \\ \ddot{\mathbf{x}}_g[k-m] \end{Bmatrix} \in \mathbf{R}^{mp \times 1} \quad (14)$$

$$\bar{\mathbf{A}}_d = \begin{Bmatrix} \mathbf{C}_f \\ \mathbf{C}_f \mathbf{A}_d^{-1} \\ \vdots \\ \mathbf{C}_f \mathbf{A}_d^{-(m-1)} \end{Bmatrix} \in \mathbf{R}^{qm \times 2n} \quad (15)$$

$$\bar{\mathbf{B}}_d = \begin{bmatrix} \mathbf{0} & \mathbf{0} & \mathbf{0} & \cdots & \mathbf{0} \\ \mathbf{0} & -\mathbf{C}_f \mathbf{A}_d^{-1} \mathbf{B}_d & \mathbf{0} & \cdots & \mathbf{0} \\ \vdots & \vdots & \vdots & \vdots & \vdots \\ \mathbf{0} & -\mathbf{C}_f \mathbf{A}_d^{-(m-1)} \mathbf{B}_d & -\mathbf{C}_f \mathbf{A}_d^{-(m-2)} \mathbf{B}_d & \cdots & -\mathbf{C}_f \mathbf{A}_d^{-1} \mathbf{B}_d \end{bmatrix} \in \mathbf{R}^{qm \times mr} \quad (16)$$

$$\bar{\mathbf{E}}_d = \begin{bmatrix} \mathbf{0} & \mathbf{0} & \mathbf{0} & \cdots & \mathbf{0} \\ \mathbf{0} & -\mathbf{C}_f \mathbf{A}_d^{-1} \mathbf{E}_d & \mathbf{0} & \cdots & \mathbf{0} \\ \vdots & \vdots & \vdots & \vdots & \vdots \\ \mathbf{0} & -\mathbf{C}_f \mathbf{A}_d^{-(m-1)} \mathbf{E}_d & -\mathbf{C}_f \mathbf{A}_d^{-(m-2)} \mathbf{E}_d & \cdots & -\mathbf{C}_f \mathbf{A}_d^{-1} \mathbf{E}_d \end{bmatrix} \in \mathbf{R}^{qm \times mp} \quad (17)$$

in which p is the number of independent excitation components and a vector or a matrix with an over bar in the above equations indicates an augmented vector or matrix. The vector $\bar{\mathbf{y}}[k-1]$ contains the sensor measurements taken at the previous m time steps, namely, the k^{th} , $(k-1)^{\text{th}}$, ..., $(k-m)^{\text{th}}$ time steps. Similarly, $\bar{\mathbf{u}} = [k-1]$ and $\bar{\mathbf{x}}_g = [k-1]$ represent the augmented vectors for the damper forces and excitations recorded from the preceding m time steps respectively. From the Eq. (11) one can determine $\mathbf{z}[k-1]$ as

$$\mathbf{z}[k-1] = \bar{\mathbf{A}}_d^{-1} (\bar{\mathbf{y}}[k-1] - \bar{\mathbf{B}}_d \bar{\mathbf{u}}[k-1] - \bar{\mathbf{E}}_d \bar{\mathbf{x}}_g[k-1]) \quad (18)$$

The matrix $\bar{\mathbf{A}}_d$ can be inverted in the earlier equation and must be non-singular. Also, the number of sensors q and the number of feedback steps m must satisfy the condition $qm = 2n$. From Eq. (18) the equation of control law of direct output feedback can be written as

$$\tilde{\mathbf{u}}[k] = \bar{\mathbf{G}}_y \bar{\mathbf{y}}[k-1] + \bar{\mathbf{G}}_u \bar{\mathbf{u}}[k-1] + \bar{\mathbf{G}}_w \bar{\mathbf{x}}_g[k-1] \quad (19)$$

where the augmented coefficient matrices may be treated as control gains and can be written as

$$\bar{\mathbf{G}}_y = \bar{\mathbf{G}}_z \bar{\mathbf{A}}_d^{-1} \quad (20)$$

$$\bar{\mathbf{G}}_z = \mathbf{K}_b \mathbf{D} (\mathbf{A}_d - \mathbf{I}) \quad (21)$$

$$\bar{\mathbf{G}}_u = -\bar{\mathbf{G}}_z \bar{\mathbf{A}}_d^{-1} \bar{\mathbf{B}}_d + \bar{\mathbf{G}}_u \mathbf{D}_1 \quad (22)$$

$$\bar{\mathbf{G}}_w = -\bar{\mathbf{G}}_z \bar{\mathbf{A}}_d^{-1} \bar{\mathbf{E}}_d + \bar{\mathbf{G}}_w \mathbf{D}_2 \quad (23)$$

where \mathbf{K}_b is a $r \times r$ diagonal matrix whose i^{th} diagonal stiffness element $k_{b,i} = 3 k_{s,i}$ of the i^{th} damper; $\mathbf{D}_1 = [\mathbf{I}_1, \mathbf{0}, \dots, \mathbf{0}] \in \mathbf{R}^{r \times mr}$, $\mathbf{D}_2 = [\mathbf{I}_2, \mathbf{0}, \dots, \mathbf{0}] \in \mathbf{R}^{p \times mp}$, $\mathbf{I}_1 \in \mathbf{R}^{r \times r}$ and $\mathbf{I}_2 \in \mathbf{R}^{p \times p}$. Once $\tilde{\mathbf{u}}[k]$ is determined by Eq. (19),

the controllable clamping force $N_i[k](i=1-r)$ for each semi-active damper can be computed by substituting each element $\tilde{u}_i[k]$ of $\tilde{\mathbf{u}}[k]$ into the Eq. (7).

The damper control force evaluated from Eq. (19) is termed as the critical damper force obtained from the predictive control law. The actual damper force considered is multiplied by the factor \mathbf{R}_f expressed by

$$\mathbf{u}[k] = \mathbf{R}_f(\bar{\mathbf{G}}_y \bar{\mathbf{y}}[k-1] + \bar{\mathbf{G}}_u \bar{\mathbf{u}}[k-1] + \bar{\mathbf{G}}_w \bar{\mathbf{x}}_g[k-1]) \quad (24)$$

In Eq. (24), the applied control force depends on the value of gain multiplier parameter \mathbf{R}_f . The parameter \mathbf{R}_f is so selected that performance of the damper in controlling the response is the best. Further, the delay in the control force between computation and actual application is neglected but its effects for a specific case are independently investigated.

4. Numerical study

To evaluate the performance of variable frictional damper, numerical examples of five and ten-storied buildings are evaluated. The properties of five and ten-story buildings (with each identical stories) considered are: (a) for the five story building the mass, stiffness and damping ratio of each story are $m_{s,i} = 11213$ kg, $k_{s,i} = 21860$ kN/m and $\xi_i = 5\%$, respectively for ($i = 1, 2, \dots, 5$) with first three natural frequencies as 2, 5.83, and 9.09 Hz and (b) for the ten story building the mass, stiffness and damping ratio of each story are $m_{s,i} = 11213$ kg, $k_{s,i} = 19820$ kN/m and $\xi_i = 5\%$, respectively for ($i = 1, 2, \dots, 10$) having first three natural frequencies as 1, 2.98, and 4.80 Hz. The seismic responses of both the buildings are investigated for four different strong earthquake ground motions namely (i) S00E component of El-Centro, 1940 (Peak Ground Acceleration (PGA)=0.348g; and g is the acceleration due to gravity), (ii) N00E component of Kobe, 1995 (PGA=0.834 g), (iii) N00E component of Loma Prieta, 1989 (PGA=0.57 g) and (iv) N00E component of Northridge, 1994 (PGA=0.843 g). The displacement and acceleration response spectra of the above four earthquake ground motions for 5% of the critical damping are shown in Fig. 2. The maximum ordinates of the acceleration are 0.918 g, 2.70 g, 2.231 g and 2.137 g, occurring at the period of 0.25s, 0.35s, 0.70s and 0.65s, for El-Centro, Kobe, Loma Prieta and Northridge earthquakes, respectively. The spectra of these ground motion indicate that the ground motions are recorded on a firm soil or rock site.

The efficacy of variable friction damper by using predictive control law with direct output feedback and the influence of gain parameter \mathbf{R}_f is investigated. Initially the optimum parameter value is evaluated by varying the \mathbf{R}_f in the range from 0 to 0.99 for both five and ten-story buildings. The several possible structural control configurations with different damper deployments are considered for evaluation of the optimum parameter \mathbf{R}_f . Placing one semi-active friction damper in each floor and gradually increasing the dampers in all the floors of five-story structure. In case of the ten-story structure placing the dampers in the first three, in the first five and all the ten floors are considered. The influence of \mathbf{R}_f on the peak displacement, absolute acceleration, base shear and peak control force are shown in Figs. 3 to 7 and Figs. 8 to 10 under different earthquake ground motions for five and ten-story structures, respectively. From the Fig. 3 to 10, it is observed that the parameter \mathbf{R}_f as well as configurations of the damper placements play an important role in the response of structures. From the Fig. 3, an optimum value of parameter \mathbf{R}_f when the damper is placed at the first floor of five-story structure is found to be 0.6 for all the responses under different earthquake ground motions. Similarly,

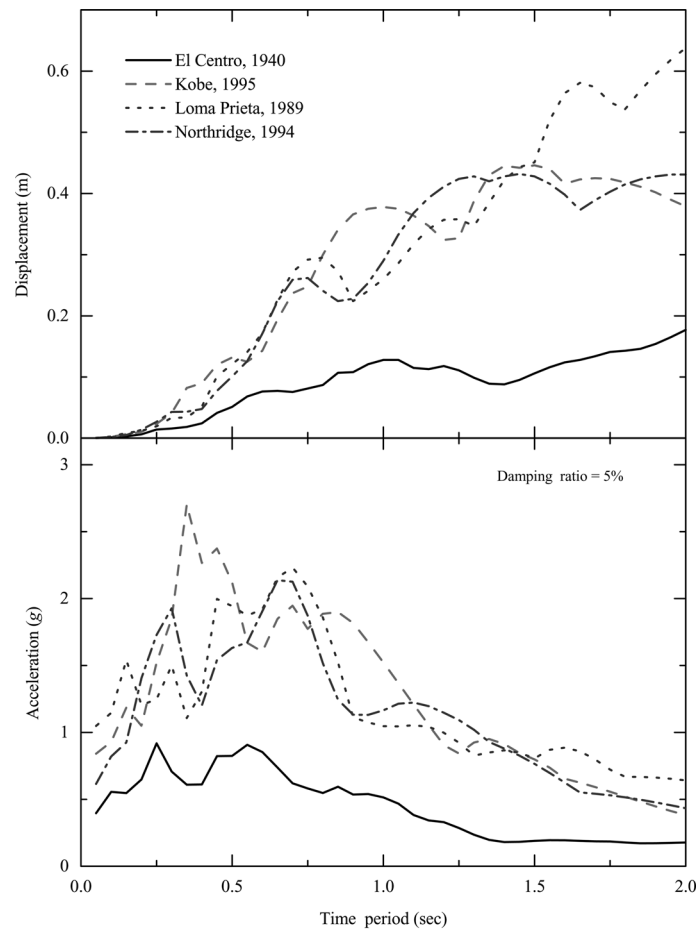


Fig. 2 Displacement and acceleration spectra of four earthquake ground motions used in analysis

the optimum parameter $R_f = 0.45, 0.5, 0.45, 0.5$ can be obtained from Figs. 4 to 7 when the dampers are placed at bottom two, three, four and all the floors of the five-story structures, respectively. The Figures 8 to 10 provide the optimum parameter R_f as 0.4, 0.55 and 0.3 for the damper placed at the bottom three, five and all the floors of ten-story structures, respectively. In addition, it is also interesting to note from the Figs. 3 to 10 that the optimum parameter R_f is not much influenced by the type of earthquake ground motion. Thus, it can be concluded that in order to produce minimum seismic structural response, the selection of optimum parameter R_f is very important and it also depends on the configuration or placement of dampers in a building.

Figs. 11 and 12 show the effectiveness of control strategy when considering changes in the properties of the semi-active dampers for five and ten-story building, respectively. In this context, the response is compared for variation in the damper friction coefficient in the range of 60% to 140%. It is observed that the displacement response of the system is relatively sensitive due to variation in the changed properties of the damper. On the other hand, the acceleration and base shear response of the system is not very sensitive due to change in the friction coefficient. Thus, even if the actual force applied to the damper is different because of the change in the frictional characteristics of the contact interface than that calculated from the predictive control will slightly alter the displacement response of the system

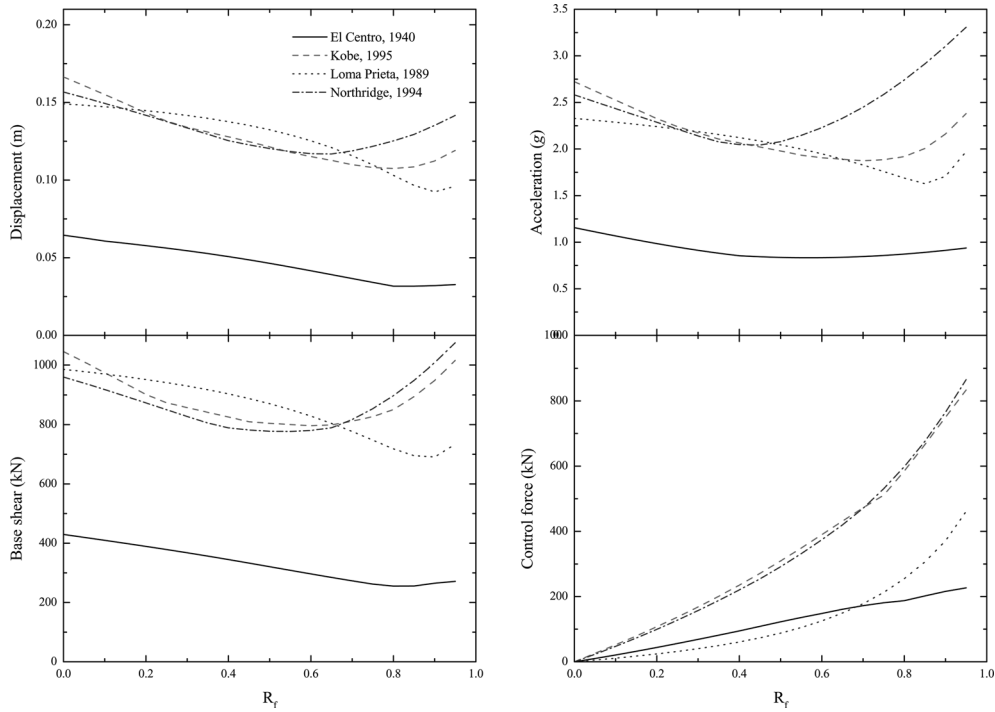


Fig. 3 Effects of R_f when semi-active damper placed at first floor of 5-story structure subjected to different earthquake ground motions

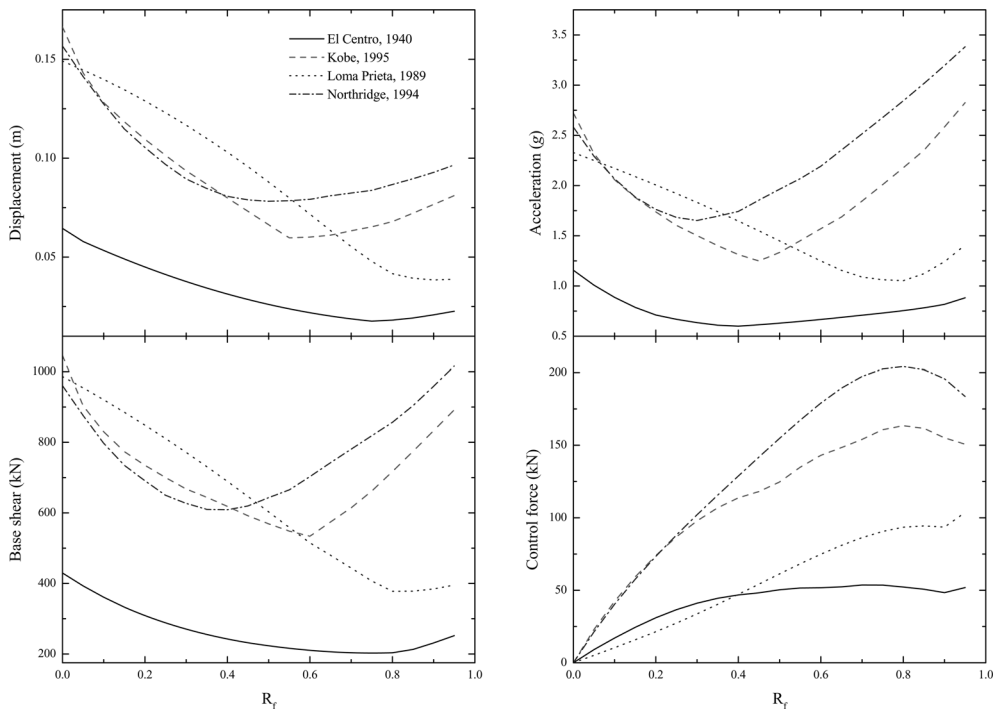


Fig. 4 Effects of R_f when semi-active damper placed at bottom two floors of 5-story structure subjected to different earthquake ground motions

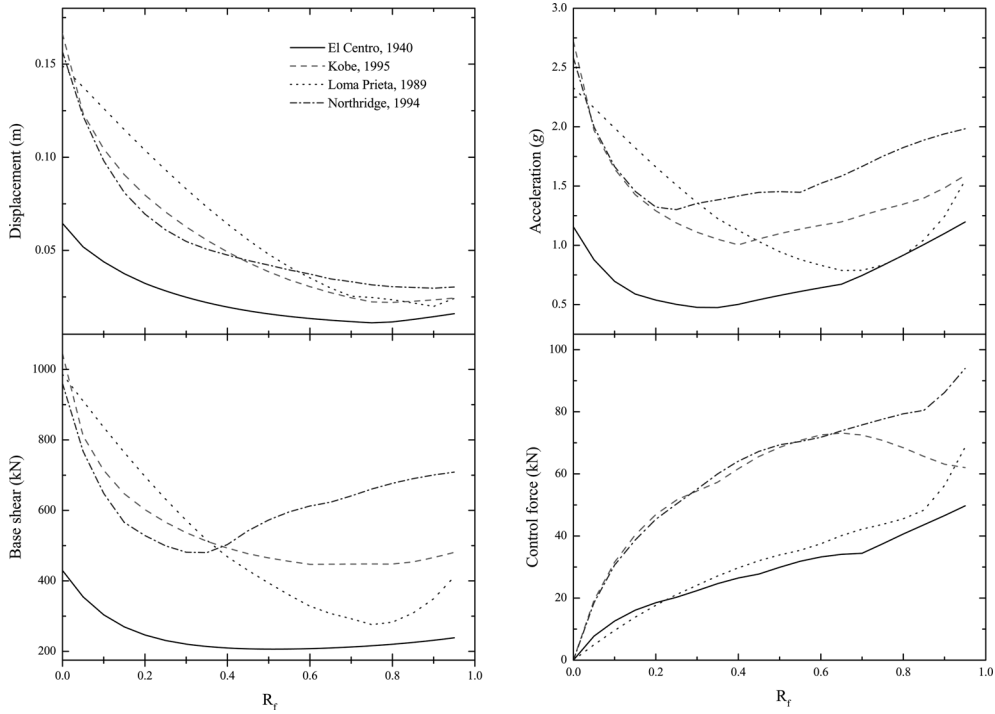


Fig. 5 Effects of R_f on peak displacement, acceleration, base shear and control force when semi-active damper placed at bottom three floors of 5-story structure subjected to different earthquake ground motions

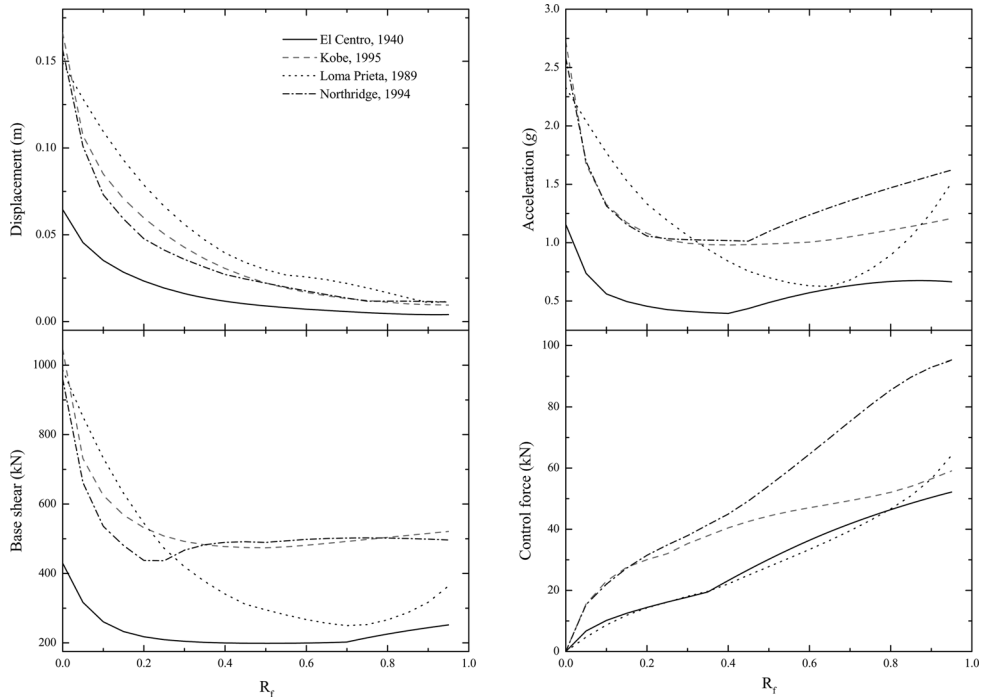


Fig. 6 Effects of R_f when semi-active damper placed at bottom four floors of 5-story structure subjected to different earthquake ground motions

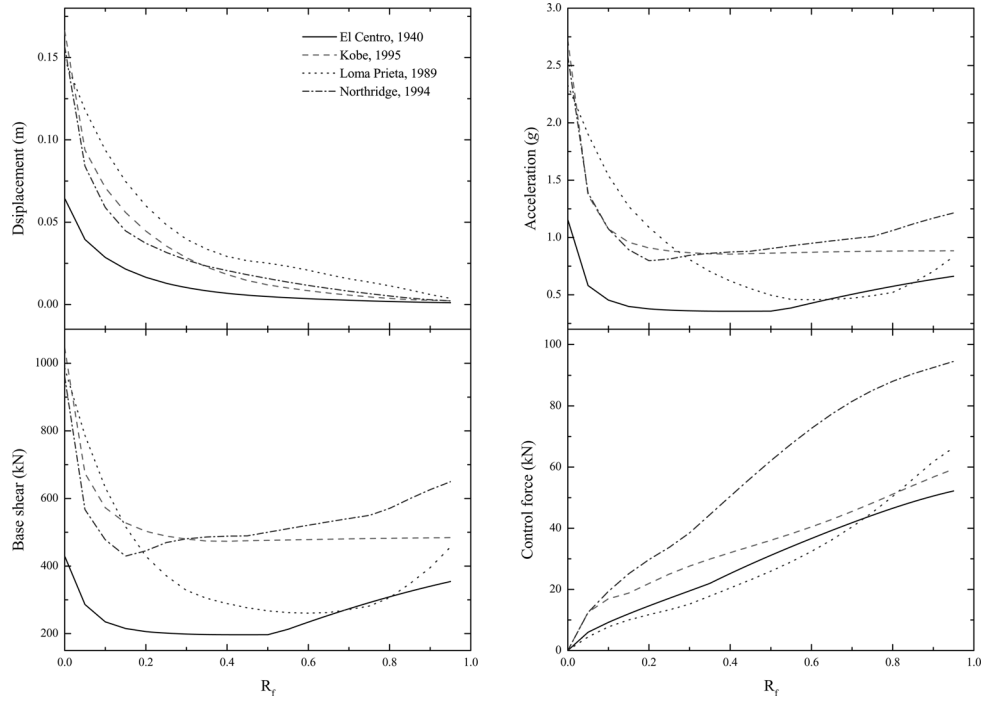


Fig. 7 Effects of R_f when semi-active damper placed at all floors of 5-story structure subjected to different earthquake ground motions

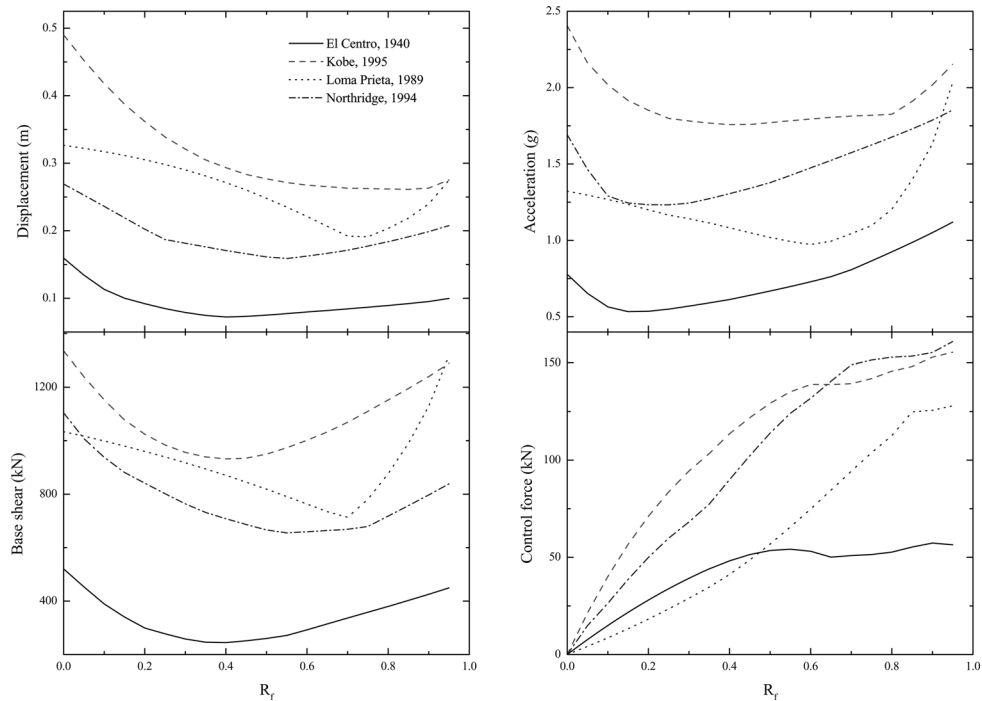


Fig. 8 Effects of R_f when semi-active damper placed at bottom three floors of 10-story structure subjected to different earthquake ground motions

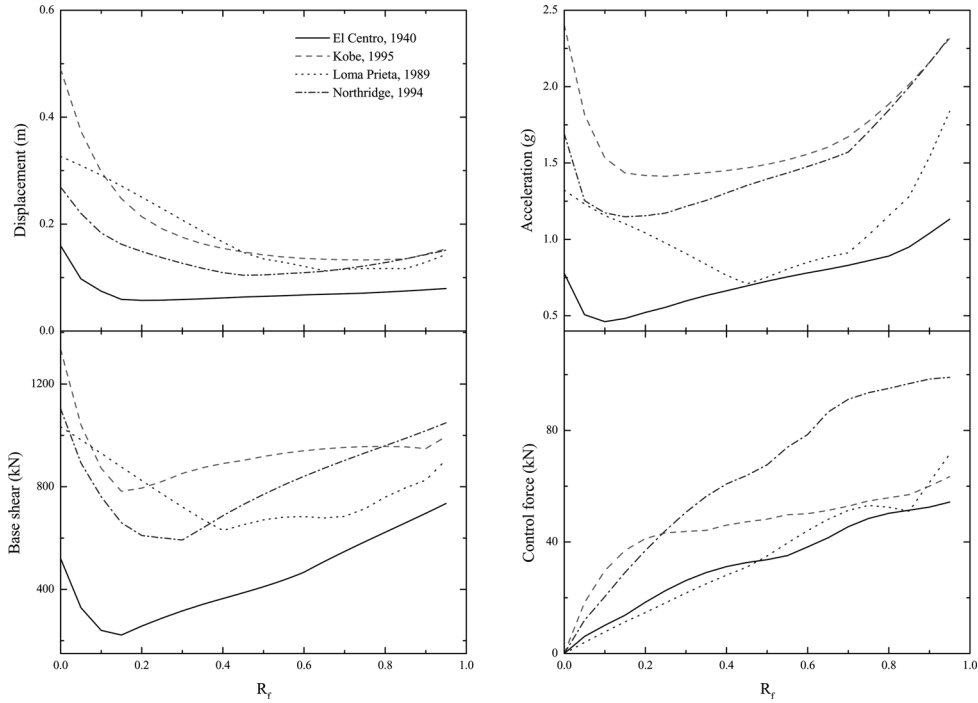


Fig. 9 Effects of R_f when semi-active damper placed at bottom five floors of 10-story structure subjected to different earthquake ground motions

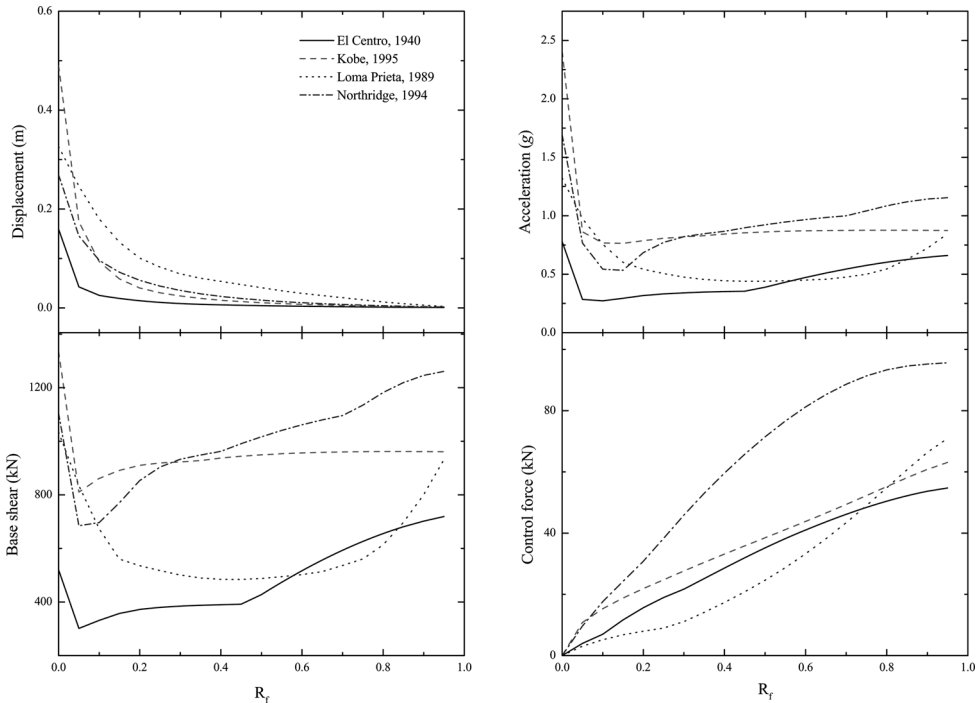


Fig. 10 Effects of R_f when semi-active damper placed at all floors of 10-story structure subjected to different earthquake ground motions

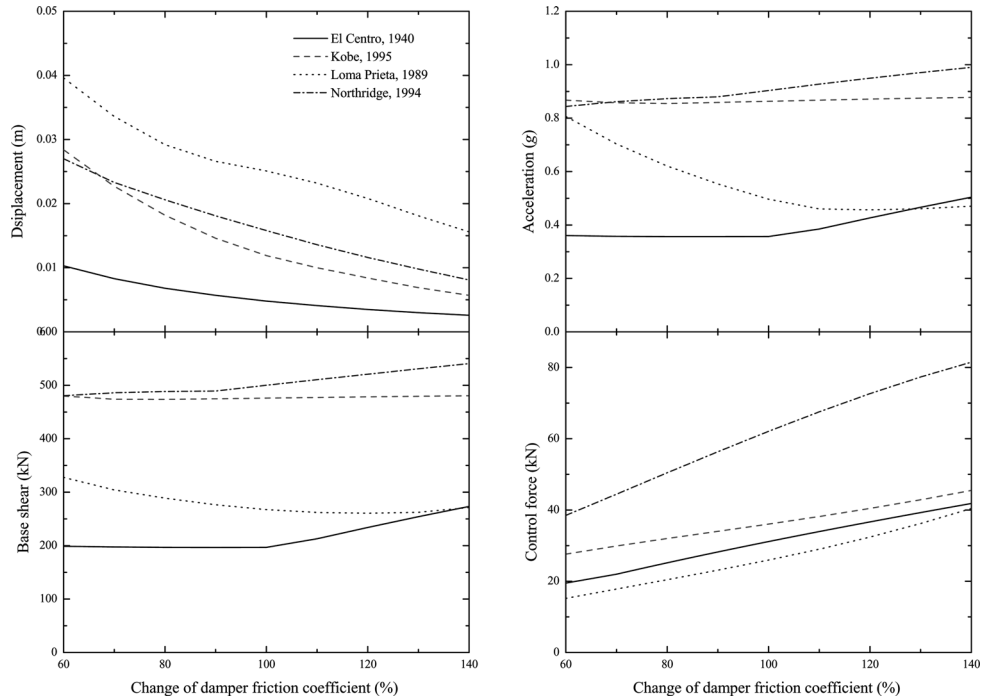


Fig. 11 Effects of percentage variation in the friction coefficient of semi-active damper placed at all floors of 5-story structure subjected to different earthquake ground motions ($R_f = 0.5$)

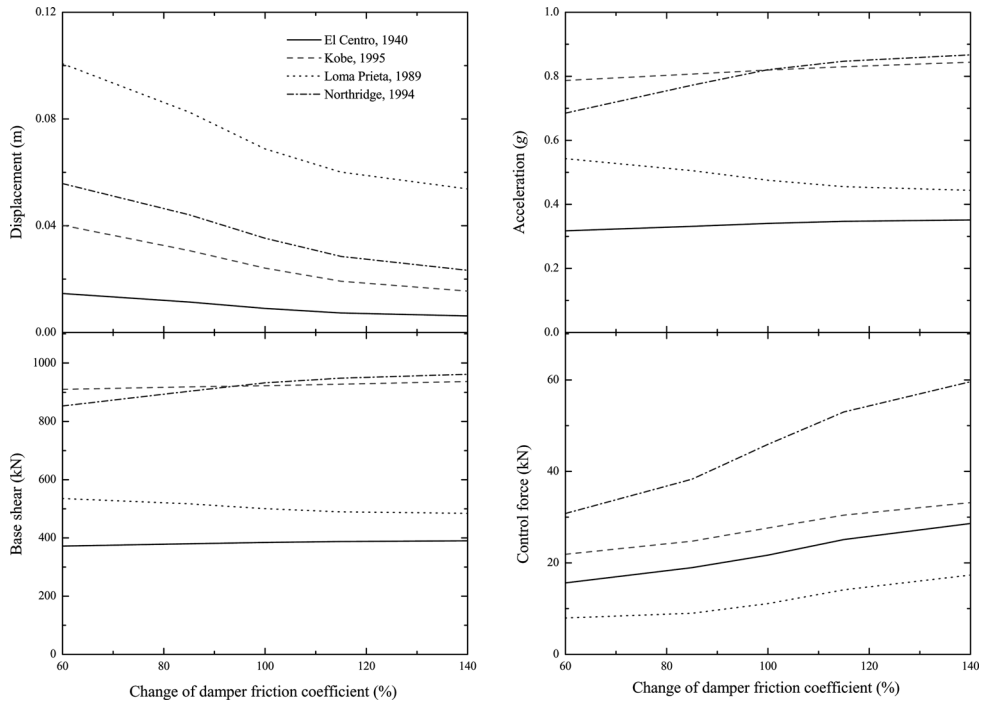


Fig. 12 Effects of percentage variation in the friction coefficient of semi-active damper placed at all floors of 10-story structure subjected to different earthquake ground motions ($R_f = 0.35$)

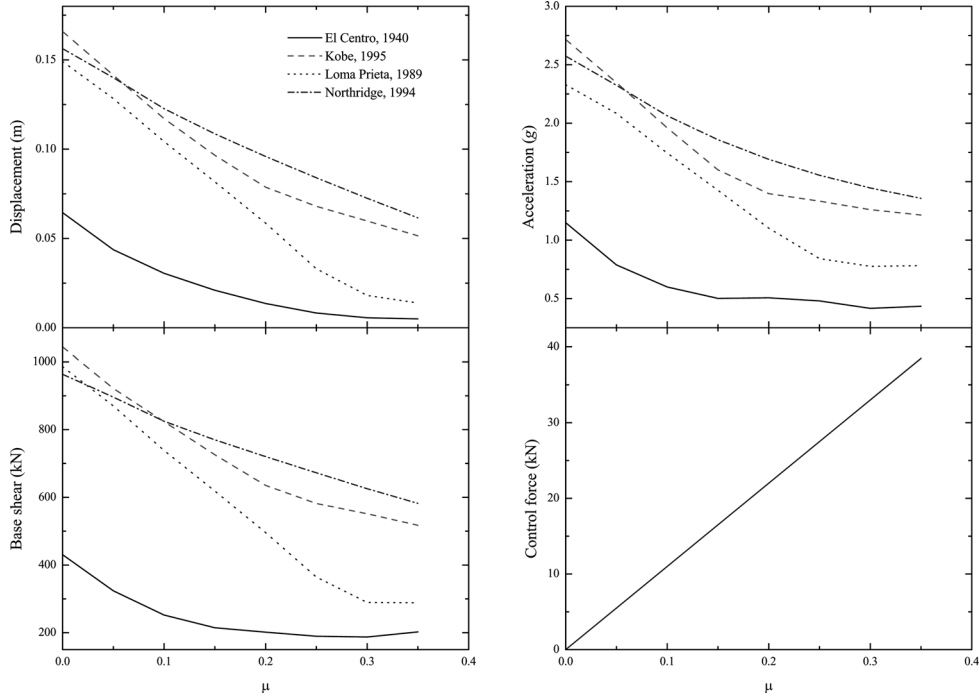


Fig. 13 Effects of coefficient of friction (μ) when passive friction damper placed at all floors of 5-story structure subjected to different earthquake ground motions

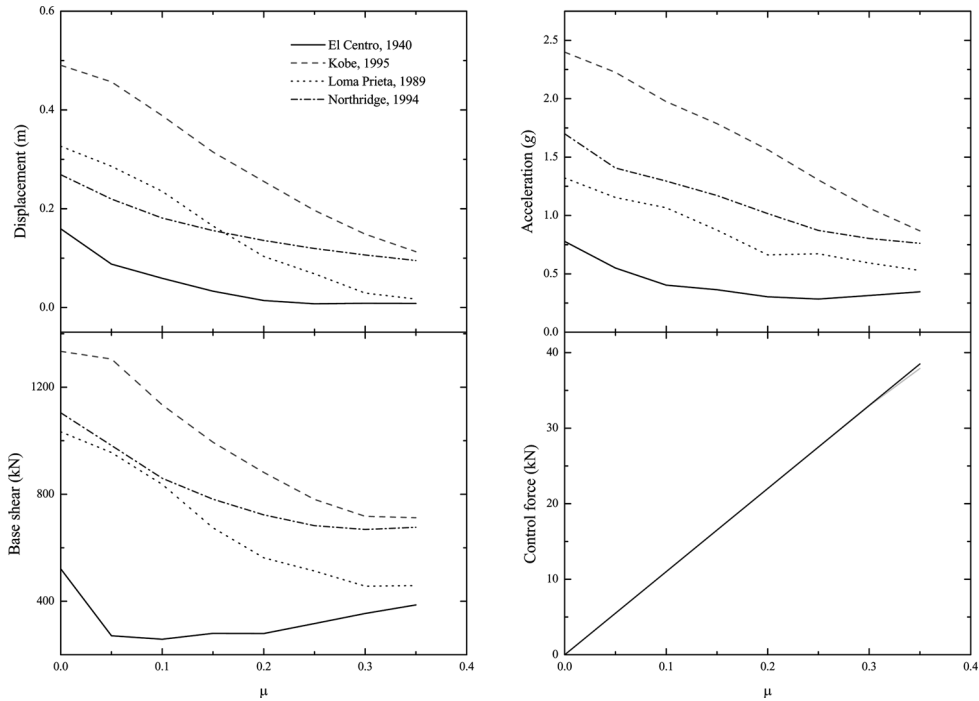


Fig. 14 Effects of coefficient of friction (μ) when passive friction damper placed at all floors of 10-story structure subjected to different earthquake ground motions

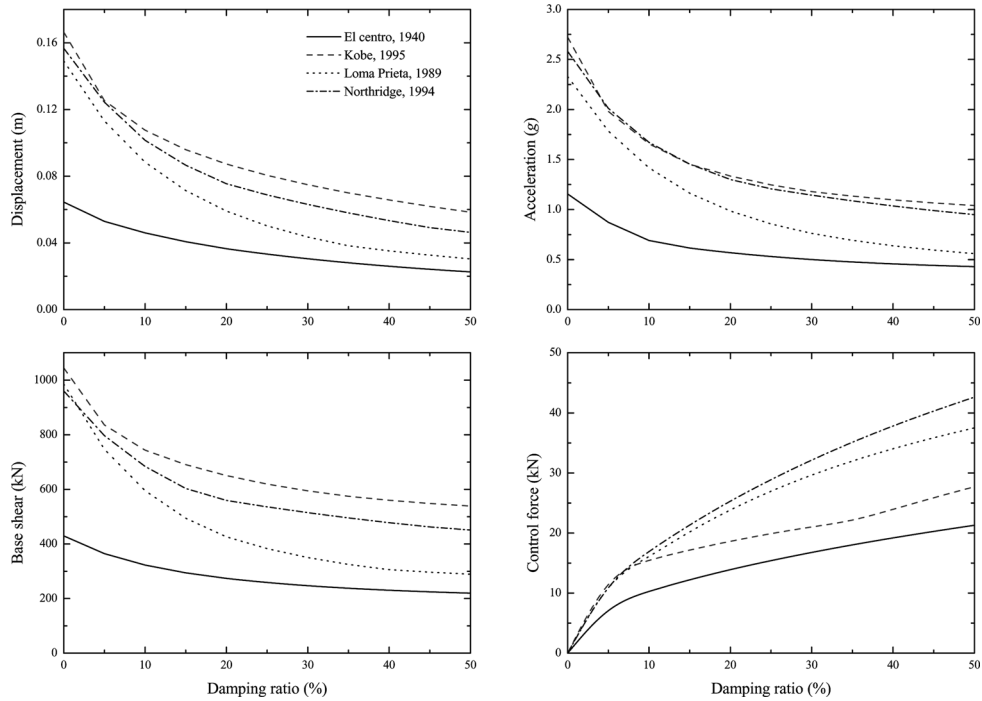


Fig. 15 Effects of damping ratio (ξ) when passive viscous damper placed at all floors of 5-story structure subjected to different earthquake ground motions

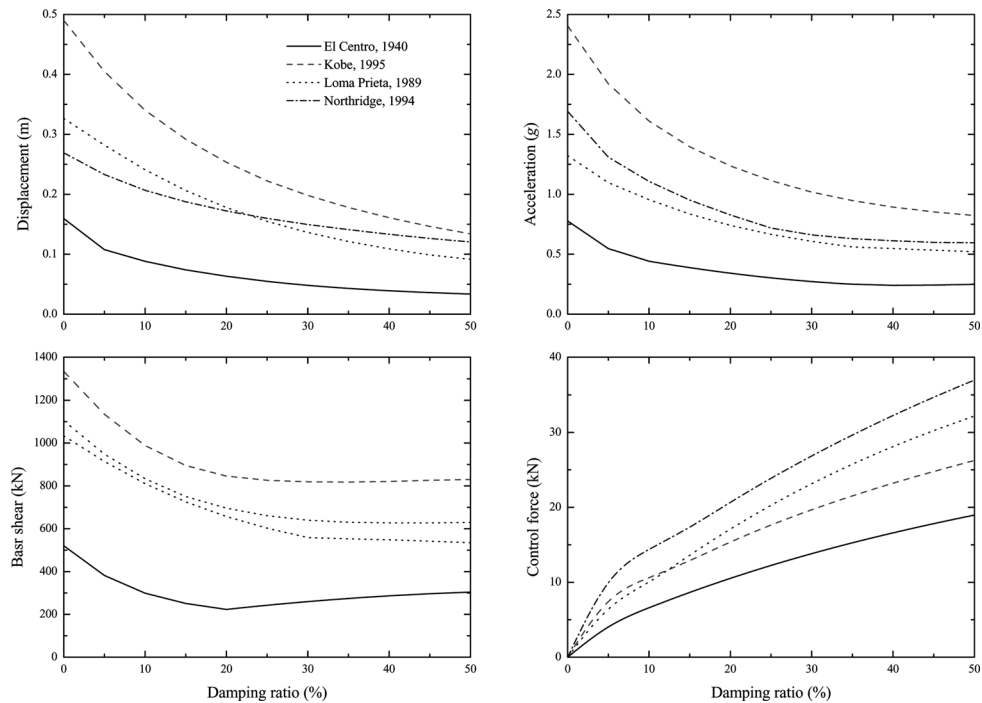


Fig. 16 Effects of damping ratio (ξ) when passive viscous damper placed at all floors of 10-story structure subjected to different earthquake ground motions

but not on the acceleration response of the system.

Figs. 13 and 14 show the effects of coefficient of friction in corresponding passive friction damper under different ground motions for five and ten story structures, respectively. These figures indicate that the optimum value for the coefficient of friction in passive friction damper can be identified as 0.3 and 0.25 for five and ten-story structures, respectively. It is also observed from these figures that the maximum passive damper force remains a fixed value under different ground motions. Similarly, Figs. 15 and 16 show parametric study for the identification of optimum value for the damping ratio of passive viscous damper. These figures indicate that the optimum value for damping ratio of passive viscous damper can be identified as 25% and 20% for five and ten story structures, respectively. The comparison of the optimal response of passive damper with that of variable friction damper indicates that the optimally designed semi-active damper performed better than the corresponding optimal passive damper.

The typical damper force-displacement relationship for different percentage optimum values of R_f are plotted in Fig. 17 in comparison with passive viscous damper. It is observed from these hysteresis loops that the damper with optimum value of R_f (i.e. 100% of R_f) shows better energy dissipation as compared to the other values. Under this condition, the shape of the loop resembles that of a viscous damper. Thus, from the parametric study it is concluded that by selecting the appropriate value of R_f in the present control law, the responses of structures can be controlled very effectively by using variable friction damper. It will be interesting to investigate the effects of time delay between the response measurement and the control action. Figs. 18 and 19 show responses of the structures against the time

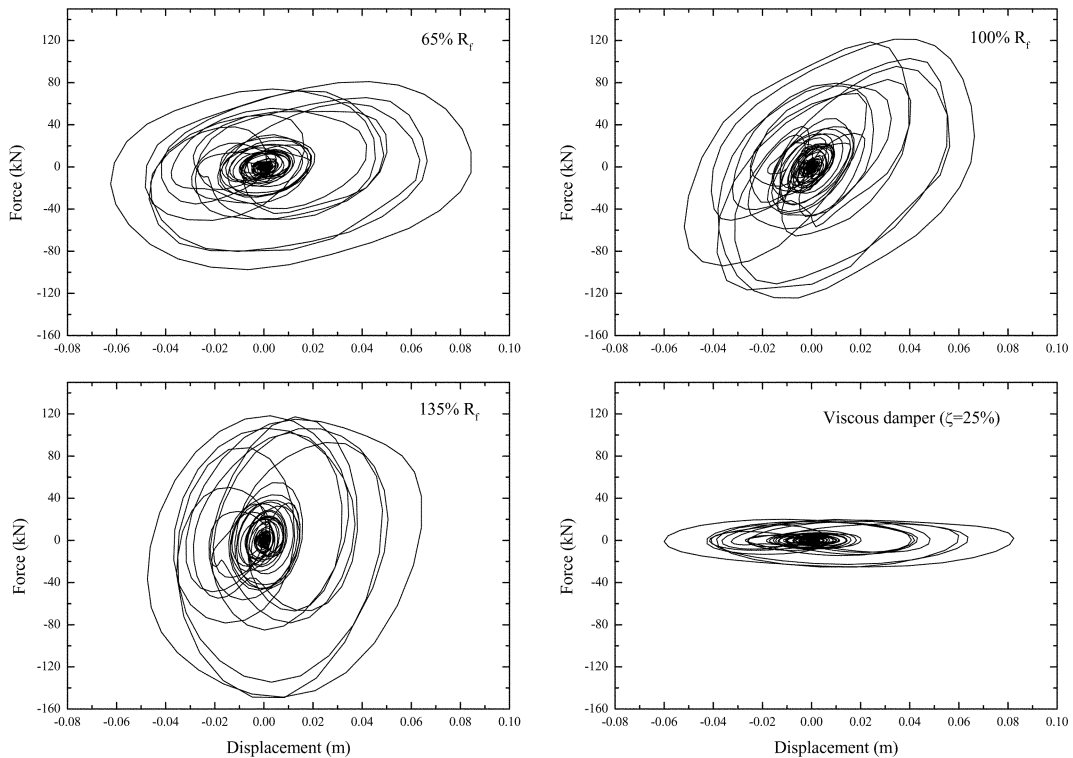


Fig. 17 Comparison of viscous damper control force-displacement diagram with different percentage optimum R_f ratio when dampers placed at bottom two floors of 5-story structure under Kobe, 1995 earthquake

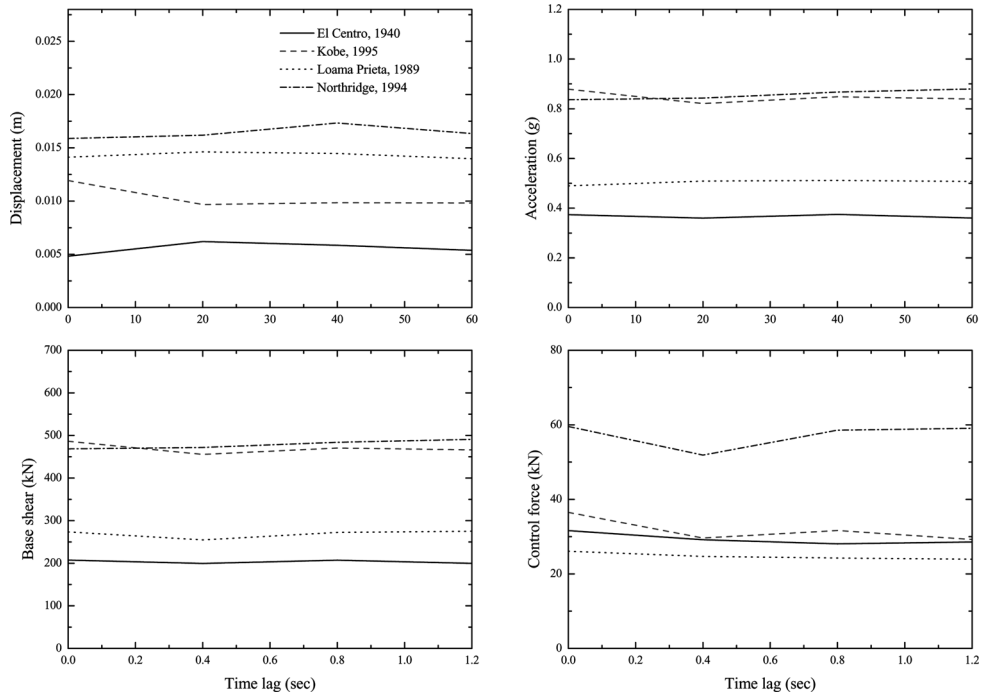


Fig. 18 Effects of time delay between the response measurement and control action when semi-active damper placed at all floors of 5-story structure subjected to different earthquake ground motions ($R_f = 0.5$)

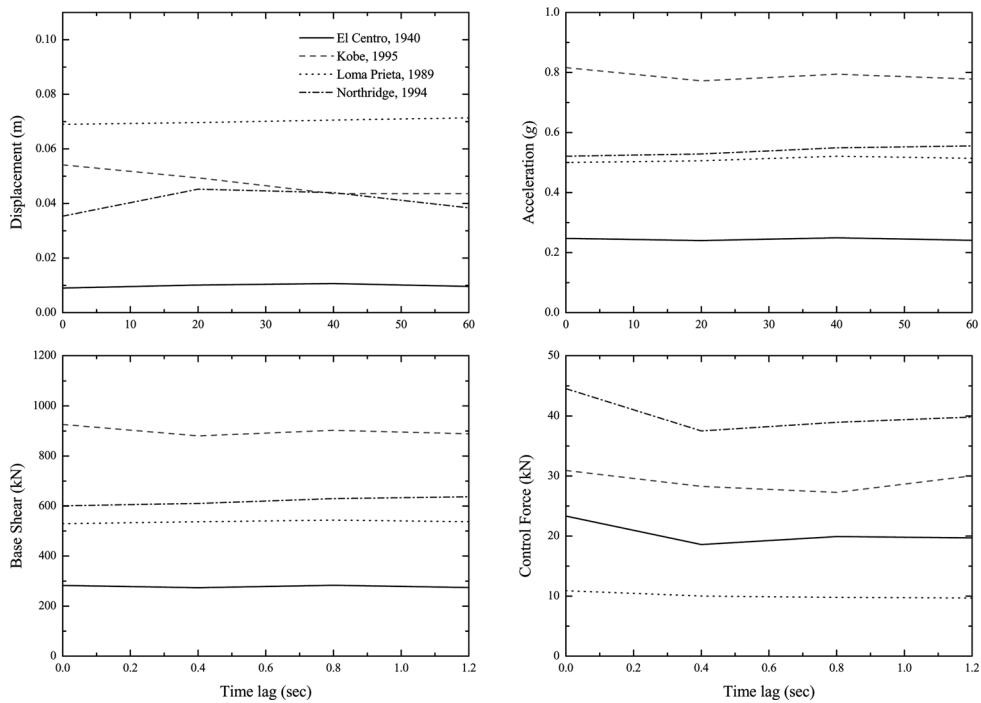


Fig. 19 Effects of time delay between the response measurement and control action when semi-active damper placed at all floors of 10-story structure subjected to different earthquake ground motions ($R_f = 0.35$)

Table 1 Comparison of 5-story structural peak responses and control forces for different control cases due to El Centro, 1940 earthquake

Control Type	Damper Placed at	Displacement (cm)					Acceleration (g)					Max. Damper Force (kN)				
		5F	4F	3F	2F	1F	5F	4F	3F	2F	1F	5F	4F	3F	2F	1F
Uncontrolled	-	6.45	5.95	4.95	3.64	1.96	1.15	1.01	0.86	0.74	0.56	-	-	-	-	-
Passive friction damper	1F	5.26	4.84	4.03	2.88	1.46	1.05	0.86	0.74	0.65	0.51	-	-	-	-	32.93
	1,2F	3.75	3.41	2.77	1.89	0.95	0.91	0.59	0.67	0.57	0.49	-	-	-	32.93	32.93
	1,2,3F	2.36	2.11	1.65	1.13	0.57	0.78	0.61	0.52	0.42	0.48	-	-	32.93	32.93	32.93
	1,2,3,4F	1.90	1.18	0.91	0.69	0.39	0.66	0.46	0.45	0.40	0.46	-	32.93	32.93	32.93	32.93
	1,2,3,4,5F	0.94	0.69	0.56	0.41	0.27	0.51	0.39	0.38	0.39	0.39	32.93	32.93	32.93	32.93	32.93
Semi-active variable friction damper	1F	4.16 (20.91)	3.82 (21.07)	3.18 (21.09)	2.26 (21.52)	1.12 (23.28)	0.83 (20.95)	0.72 (16.28)	0.61 (17.56)	0.50 (30.56)	0.39 (23.38)	-	-	-	-	148.1
	1,2F	2.85 (24.00)	2.60 (23.75)	2.11 (23.82)	1.41 (25.37)	0.73 (23.15)	0.61 (32.96)	0.50 (15.25)	0.44 (34.32)	0.37 (35.08)	0.36 (26.53)	-	-	-	103.7	48.24
	1,2,3F	1.49 (36.86)	1.37 (35.07)	0.98 (40.60)	0.63 (44.24)	0.34 (40.35)	0.57 (26.92)	0.43 (29.51)	0.36 (30.76)	0.36 (14.28)	0.37 (23.07)	-	90.38	53.22	29.89	
	1,2,3,4F	1.02 (46.31)	0.84 (28.81)	0.67 (26.37)	0.50 (27.53)	0.27 (30.76)	0.43 (34.84)	0.36 (21.74)	0.35 (22.22)	0.35 (13.79)	0.35 (23.58)	-	69.68	43.19	35.30	26.76
	1,2,3,4,5F	0.48 (48.93)	0.47 (31.88)	0.44 (21.43)	0.35 (14.63)	0.21 (22.22)	0.35 (31.37)	0.35 (10.25)	0.35 (7.27)	0.35 (9.62)	0.36 (7.69)	39.6	41.24	44.10	42.75	31.13

Numbers in parentheses denote the % reduction in responses compared to the Passive control system

delay under different earthquake ground motions for 5 and 10 story buildings, respectively. It is observed that the delay in the control force will not significantly change the response of structures.

Several possible structural control configurations with different damper deployments for uncontrolled structure without adding any damper, controlled structure with passive/semi-active dampers for both five and ten-story structures are investigated. It is to be noted that the presented results, including those for uncertainties in properties and time delay effects, are based on the assumption of continuous sliding of the semi-active friction device. This assumption requires precise knowledge of the friction force, which is not possible, or monitoring of response and feedback to ensure continuous sliding, which has not been considered in this paper. Table 1 summarizes the maximum values of the floor displacements, floor accelerations as well as the damper forces resulted from the all five cases of five-story structures are evaluated under the El-Centro (1940) earthquake ground motion. Note that in Table 1 the control parameter R_f is considered for semi-active damper based on the optimum values of damper deployments in the five-story structure. The structural responses and control forces for all five cases are presented in Table 1 the numbers in parentheses denotes the percentage reduction in responses with the passive control system. From Table 1 it is observed that by increasing the dampers from the bottom story to top story at regular interval, both for passive and semi-active dampers creates a considerable reduction in structural responses is obtained. Further, it is also important to note that increasing the number of semi-active dampers is not desirable from the economical point of view. Hence, by comparing results from Table 1, it can be seen that with a minimum two semi-active dampers more effective control of the structural responses in the five-story structure can be achieved. Based on this conclusion, further study is also made for other real earthquake ground motion i.e., Kobe (1995), Loma Prieta (1989) and Northridge (1994) and the results are tabulated in Table 2. The corresponding results for the ten-story structure by placing the dampers at first three floors, first five floors and all the floors are tabulated in Table 3. From Table 3, it is observed that a minimum of five variable friction semi-active dampers are

Table 2 Comparison of 5-story peak structural responses under different ground motions

Control Type	Damper Placed at	Gain multiplier (R_f)	Displacement (cm)				Acceleration (g)			
			El Centro (1940)	Kobe (1995)	Loma-Prieta (1989)	Northridge (1994)	El Centro (1940)	Kobe (1995)	Loma-Prieta (1989)	Northridge (1994)
Uncontrolled	-	-	6.45	16.64	14.91	15.57	1.15	2.72	2.32	2.58
Passive friction damper	1F	-	5.26	15.50	14.22	14.66	1.05	2.56	2.28	2.43
	1,2F	-	3.75	13.13	12.29	13.32	0.91	2.32	2.13	2.16
	1,2,3F	-	2.36	10.28	9.19	11.21	0.78	1.94	1.80	1.83
	1,2,3,4F	-	1.90	7.60	6.44	9.24	0.66	1.44	1.22	1.54
	1,2,3,4,5F	-	0.94	4.69	2.59	5.25	0.51	1.26	0.77	1.44
Semi-active Variable friction damper	1F	0.6	4.16 (20.91)	11.51 (25.74)	12.53 (11.88)	11.70 (20.19)	0.83 (20.95)	1.90 (25.78)	1.94 (14.91)	2.12 (12.75)
	1,2F	0.45	2.85 (24.00)	7.31 (44.32)	9.57 (22.13)	7.89 (40.01)	0.61 (32.96)	1.24 (46.55)	1.54 (27.69)	1.85 (14.35)
	1,2,3F	0.5	1.49 (36.86)	3.85 (62.54)	4.79 (47.87)	4.21 (62.44)	0.57 (26.92)	1.09 (43.81)	0.94 (47.77)	1.45 (20.76)
	1,2,3,4F	0.45	1.02 (46.31)	2.60 (65.79)	3.40 (47.50)	3.40 (63.20)	0.43 (34.84)	0.98 (31.94)	0.75 (38.52)	1.01 (34.41)
	1,2,3,4,5F	0.5	0.48 (48.93)	1.19 (74.62)	1.41 (45.56)	1.58 (69.90)	0.35 (31.37)	0.86 (31.74)	0.49 (36.36)	0.90 (37.71)

Numbers in parentheses denote the % reduction in responses compared to the Passive control system

Table 3 Comparison of 10-story peak structural responses under different ground motions

Control Type	Damper Placed at	Gain multiplier (R_f)	Displacement (cm)				Acceleration (g)			
			El Centro (1940)	Kobe (1995)	Loma-Prieta (1989)	Northridge (1994)	El Centro (1940)	Kobe (1995)	Loma-Prieta (1989)	Northridge (1994)
Uncontrolled	-	-	15.95	49.01	32.65	26.92	0.77	2.40	1.32	1.69
Passive friction damper	1,2,3F	-	10.60	45.68	30.14	23.84	0.67	2.21	1.31	1.52
	1,2,3,4,5F	-	7.28	39.89	26.29	18.67	0.54	2.11	1.30	1.18
	All Floors	-	2.15	19.67	17.83	11.96	0.41	1.30	0.67	0.87
Semi-active variable friction damper	1,2,3F	0.4	7.22 (31.88)	29.35 (35.74)	27.12 (10.09)	17.07 (28.39)	0.51 (23.58)	1.75 (20.81)	1.08 (17.40)	1.30 (14.14)
	1,2,3,4,5F	0.55	4.60 (36.81)	13.84 (65.30)	12.86 (53.25)	10.71 (42.63)	0.40 (25.92)	1.52 (27.96)	0.80 (38.46)	0.92 (22.03)
	All Floors	0.3	0.9 (58.13)	5.41 (72.49)	6.88 (61.41)	3.53 (70.48)	0.24 (41.46)	0.81 (37.69)	0.49 (41.79)	0.52 (40.22)

Numbers in parentheses denotes the % reduction in responses compared to the Passive control system

found more effective in all cases of real ground motions as compared to multiple passive friction dampers. The results from Table 3 also indicate that with a minimum of five semi-active variable friction dampers it is possible to reduce the responses by about 30% to 40% in comparison with passive friction dampers under different real ground motion for the ten-story structure.

Figs. 20 and 21 compare the time variation of the top story displacements, the absolute top story acceleration and base shear of the uncontrolled structure, structure with first five floors with passive dampers/ semi-active dampers under the real ground motion of the Northridge (1994) in the five and ten story structures respectively by choosing appropriate evaluated value of R_f . It can be observed from

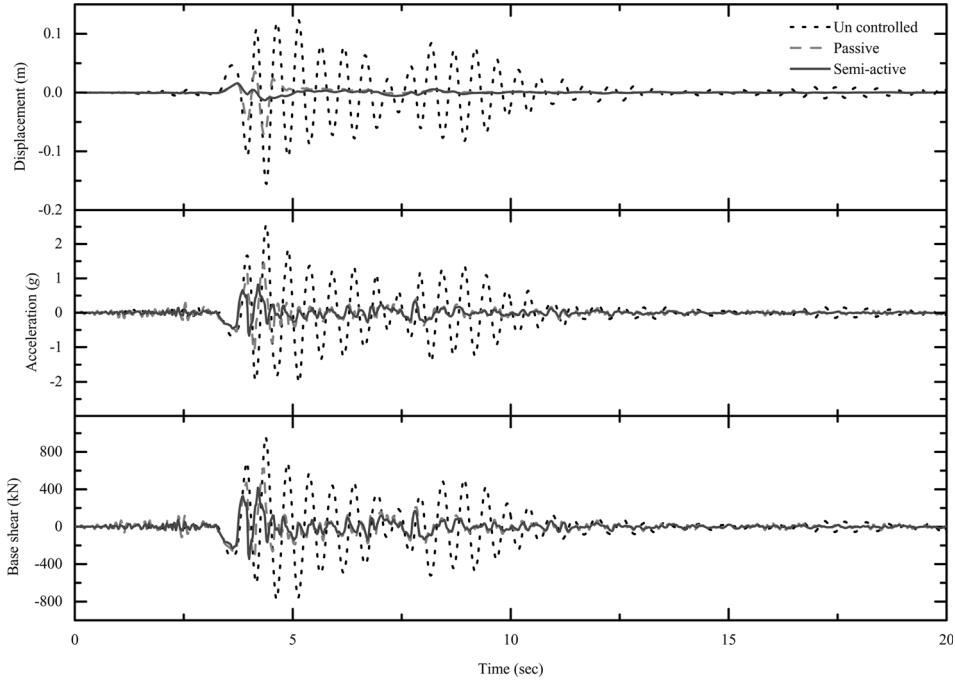


Fig. 20 Time variation of top floor displacement, acceleration and base shear of the Uncontrolled, Passive and Semi-active friction dampers placed at all the floors of 5-story structure under Northridge, 1994 earthquake

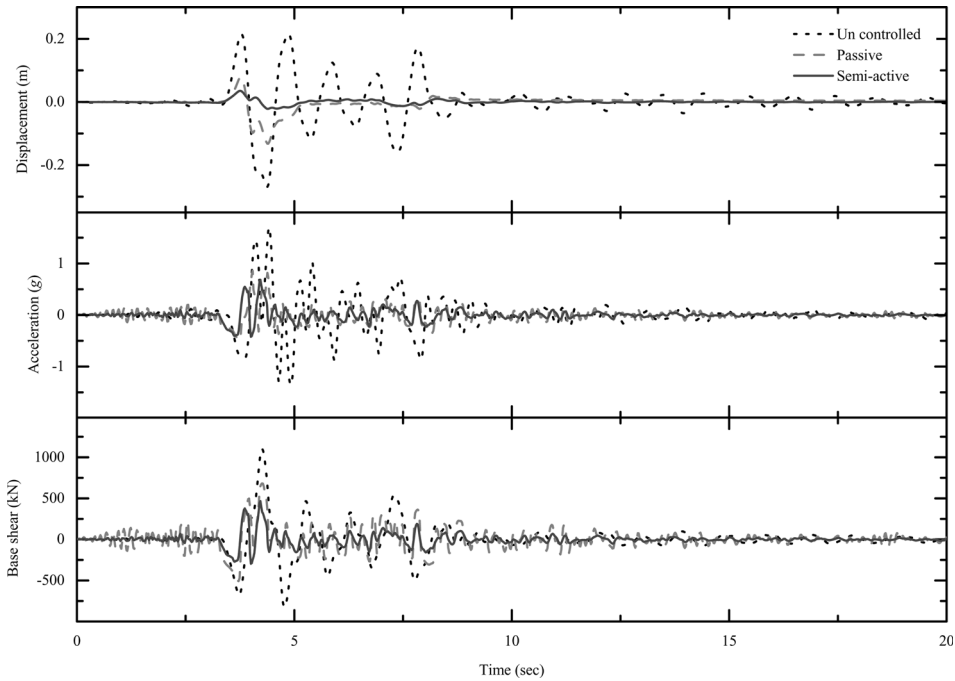


Fig. 21 Time variation of top floor displacement, acceleration and base shear of the Uncontrolled, Passive and Semi-active friction dampers placed at bottom five floors of 10-story structure under Northridge, 1994 earthquake

the Figs. 20 and 21 that the semi-active dampers provides the most effective reduction in the displacement, acceleration and base shear as compared to passive dampers.

5. Conclusions

The effectiveness and performance of seismic structures with semi-active variable friction dampers is presented. Five and ten-story structures with several possible structural configurations with passive and semi-active dampers under four real earthquake ground motions are studied. The optimal parameter \mathbf{R}_f of predictive control algorithm is evaluated for different configuration of damper deployments, which plays an important role in the present control algorithm. The variable slip force of a semi-active friction damper is kept slightly lower than the critical friction force that allows the damper to remain in slip state during an earthquake, improving the energy dissipation capacity of the damper. The control algorithm is able to produce continuous and smooth slip force for variable friction dampers. Based on the results of numerical investigations, the following conclusions are drawn.

1) The evaluated optimum parameter \mathbf{R}_f of the predictive control law for the variable semi-active friction damper is found satisfactory in reducing the structural responses considerably for the selected structures under four different earthquake ground motions.

2) For the semi-active variable friction damper to remains in slip state and produce minimum structure response, the optimum parameter \mathbf{R}_f depends on configuration and placement of dampers at which maximum energy dissipation occurs.

3) The larger value of \mathbf{R}_f produces higher control force but for the different configurations of the damper locations it is always not effective in reducing the structural response.

4) The multi-level semi-active variable friction dampers reduced the structural response considerably as compared to passive friction devices but from the economical point of view, it is not desirable. Thus, with the minimum number of semi-active variable friction dampers, it is possible to reduce the peak responses by about 30 to 40 percent under different real ground motions as compared to the corresponding passive friction devices.

5) The optimum value of \mathbf{R}_f produces continuous smooth slip forces and the maximum hysteretic energy dissipation is in the controlled structure.

6) The optimal semi-active variable friction dampers are more effective in reducing displacements, accelerations and base shear of the structures as compared to passive friction dampers.

References

- Akbay, Z. and Aktan, H. M. (1995), "Abating earthquake effects on building by active-slip brace devices", *Shock Vib.*, **2**, 133-142.
- Chen, C. and Chen, G. (2002), "Non-linear control of a 20-storey steel building with active piezoelectric friction dampers", *Struct. Eng. Mech.*, **14**, 21-38.
- Feng, M. Q., Shinozuka, M. and Fujii, S. (1993), "Friction controllable sliding isolation system", *J. Eng. Mech.*, ASCE, **119**, 1845-1864.
- Housner, G. W., Bergman, L. A., Caughey, T. K., Chassiakos, A. G., Claus, R. O., Masri, S. F., Skelton, R. E., Soong, T. T., Spencer, B. F. and Yao, J. T. P. (1997), "Structural control: past, present, and future", *J. Eng. Mech.*, **123**, 897-971.
- Inaudi, J. A. (1997), "Modulated homogeneous friction: a semi-active damping strategy", *Earthq. Eng. Struct. Dyn.*,

- 26, 361-376.
- Kannan, S., Uras, H. M. and Aktan, H. M. (1995), "Active control of building seismic response by energy dissipation", *Earthq. Eng. Struct. Dyn.*, **24**, 747-759.
- Lu, L. Y. and Chung, L. L. (2001). "Model control of seismic structure using augmented state matrix", *Earthq. Eng. Struct. Dyn.*, **30**(2), 237-256.
- Lu, L. Y. (2004a), "Predictive control of seismic structures with semi-active friction dampers", *Earthq. Eng. Struct. Dyn.*, **33**, 647-668.
- Lu, L. Y. (2004b), "Semi-active model control for seismic structures with variable friction dampers", *Eng. Struct.*, **26**, 437-454.
- Lu, L. Y., Chung, L. L. and Lin, G. L. (2004), "A general method for semi-active feedback control of variable friction dampers", *J. Intell. Mater. Sys. Struct.*, **15**, 393-412.
- Meirovitch, L. (1990), "Dynamics and control of structures", John Wiley & Sons, New York.
- Sadek, F. and Mohraz, B. (1998), "Semi-active control algorithms for structures with variable dampers", *J. Eng. Mech.*, ASCE, **124**, 981-990.
- Soong, T. T. and Constantinou, M. C. (1994), *Passive and Active Structural Vibration Control in Civil Engineering*, Springer, New York.
- Soong, T. T. and Dargush, G. F. (1997), "Passive energy dissipation systems in structural engineering", Wiley, New York.
- Soong, T. T. and Spencer, B. F. Jr (2002), "Supplemental energy dissipation: state-of-the-art and state-of-the-practice", *Eng. Struct.*, **24**, 243-259.
- Soong, T. T. (1990), *Active Structural Control: Theory and Practice*. Longman, New York.
- Symans, M. D. and Constantinou, M. C. (1999), "Semi-active control system for seismic protection of structures: a state-of-the art review", *Eng. Struct.*, **21**, 469-487.
- Xu, Y. L., Qu, W. L. and Chen, Z. H. (2001), "Control of wind-excited truss tower using semi-active friction damper", *J. Struct. Eng.*, ASCE, **127**, 861-868.
- Yang, J. N. and Agrawal, A. K. (2002), "Semi-active hybrid control systems for nonlinear buildings against near-field earthquakes", *Eng. Struct.*, **24**, 271-280.

Notation

The following symbols are used in the paper:

A	: system matrix
A_d	: discrete-time system matrix
B	: distributing matrix of the control forces
B_d	: discrete-time counterpart of B matrix
C	: damping matrix of the system
C_f	: sensor placement matrix
E	: distributing matrix of the excitations
E_d	: discrete-time counterpart of E matrix
$\bar{\mathbf{G}}_u, \bar{\mathbf{G}}_w, \bar{\mathbf{G}}_y, \mathbf{G}_z$: augmented coefficient matrices
I	: identity matrix
K	: stiffness matrix of the system
K_b	: ($r \times r$) diagonal matrix
k	: time step
$k_{b,i}$: stiffness of bracing at the i -th dampers
$k_{s,i}$: story stiffness at i -th floor
$m_{s,i}$: story mass at i -th floor
M	: mass matrix of the system
N_i	: controllable clamping force at the i -th dampers
n	: number of story
q	: number of sensors

- \mathbf{R}_f : gain multiplier i.e., ratio of damper force to critical friction force
- r : total number of dampers
- $\mathbf{u}[k]$: vector of controllable friction forces
- $\tilde{\mathbf{u}}[k]$: critical force vector
- $\ddot{x}_g(t)$: vector of ground accelerations
- $x_i(t)$: story displacement relative to the ground at i -th floor
- \mathbf{y}_s : sensor measurement vector
- $\mathbf{z}(\mathbf{t})$: state vector
- Δt : time interval
- μ : frictional coefficient
- $\mathbf{1}$: influence coefficient vector

CC